Eurasian Journal of Physics and Functional Materials

2018, 2(4), 315-325

System and process of thermal neutron flux producing by means of an accelerator base electron of 18 MeV

A. Didi[1], A. Dadouch[1], H. El Bekkour[1], O. Jai[2], F.-Z. Bouhal[1], M. Bencheikh[1]

[1]University of Sidi Mohamed Ben Abdellah, Fez, Morocco

[2]Abdelmalek Essaadi University

E-mail: abdessamad.didi1@usmba.ac.ma

DOI: **10.29317/ejpfm.2018020403**
Received: 15.10.2018 - after revision

Neutrons are produced in accelerators by irradiating heavy targets with an electron or proton beam. Produced neutrons are of high energy. The purpose of our work is optimization the neutron flux by MCNP-6 code for production the thermal neutron flux using a moderator and for convertation the fast neutron flux into a thermal neutron flux. In this article, we are interested in a thermal neutron flux due it is useful for method of neutron activation analysis. In conventional sources, the moderator is usually a large volume of water or paraffin around the source. Initially, fast neutrons have energy above 1 MeV, and then slow down to energies below 1 eV.

Keywords: MCNP-6, Accelerator of particles, electron beam, neutron flux.

Introduction

Today, more than 40 million people undergo some form of nuclear medicine procedures. Generally, it's diagnosis and treatment of cancerous diseases. Despite the widespread use of radioisotopes in the world, the production of these is available only in developed countries. Although, the production of radioisotopes includes a nuclear reactor [1-5], a source of alpha-beryllium [6-8] and an accelerator

[9]. In these recent years, global demand for molybdenum radioisotopes has increased significantly, with 90% of these was producted by five old reactors located in Canada, Belgium, the Netherlands, South Africa and France. Unfortunately, these five reactors have been in the final stage of being stopped more than 50 years. Researchers have developed other production methods, which are mainly improvements in spallation neutron sources and particle accelerators [10-14].

Theoretically, the neutron flux in particle/cm^2 can be simulated using following formula [15]:

$$\phi_s = \frac{1}{A}\int dE \int dt \int dA \int d\Omega \Psi\left(\overrightarrow{r,\Omega,E,t}\right) \tag{1}$$

With, A is the surface area $\left(\text{cm}^2\right)$; E is the total energy deposited; $\left(\overrightarrow{r,\Omega,E,t}\right)$ is particle position vector (cm); direction vector, energy (MeV); and time and Ψ is angular flux generated from nuclear reactor.

Theory

The availability of the Monte Carlo MCNP-X and MCNP-6 codes used as a simulation tool [15-17] makes it possible to pretend an electron beam in thick targets X. The optimization of the conception (design) of the target bound directly to the production and the generation of the yield on Bremsstrahlung of photon neutron [18-21]. Figure 1, show the geometry used in this work. In this article, we interested in the production of neutrons using a system of acceleration of the electron beam of the energy of 18 MeV and moderation of the neutron using a water cylinder thickness of 7 cm and a diameter of 5 cm. We have devoted the study to the production of thermal neutrons using a (water). Figure 1 schematizes the device used for an accelerator base electron and the moderator used.

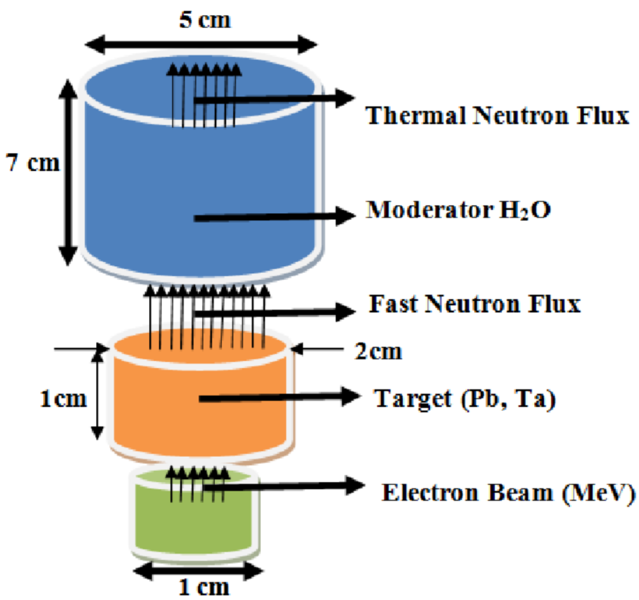

Figure 1. An electron-based accelerator and target with moderator.

Results

The thermal neutron flux generated by the Lead target

Figure 2 represents two cases; the first gives the neutron flux as a function of neutron energy with and without a moderator. In the first case, the flux is important when the energy of 0.5 MeV exceeds. On the other hand, the neutron flux is negligible, in the second case in the presence of the moderator; the flux is maximum in the region of less than 0.75 MeV.

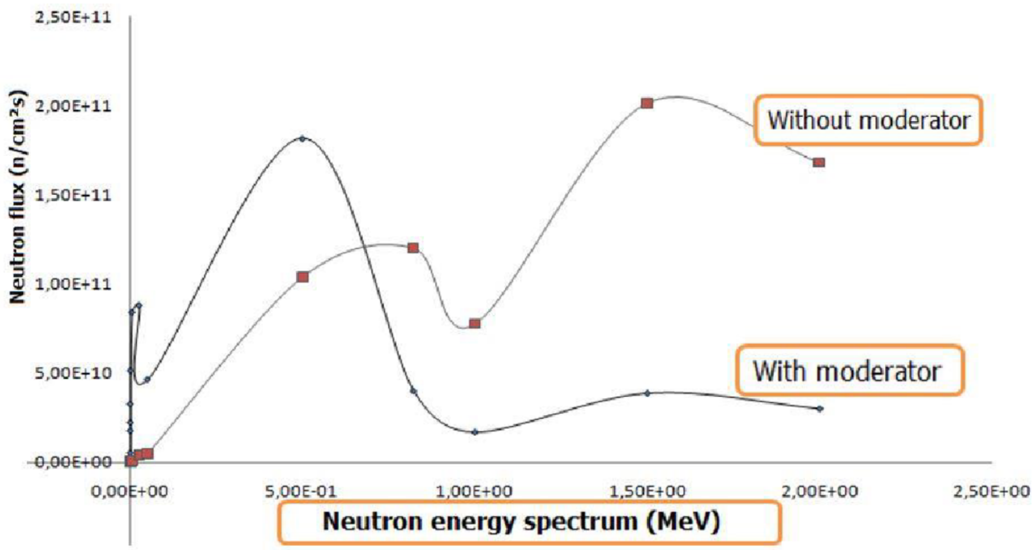

Figure 2. Neutron flux profile in cases with moderation and without moderation at low energy for target Pb.

Discretization at the level of energy groups in the thermal domain. We find Figure 3, which represents the neutron flux as a function of neutron energy in the thermal domain, clearly, that in the zone of low energy the thermal neutron flux and more intense to compare with the other the rate without a moderator or the flux is almost zero.

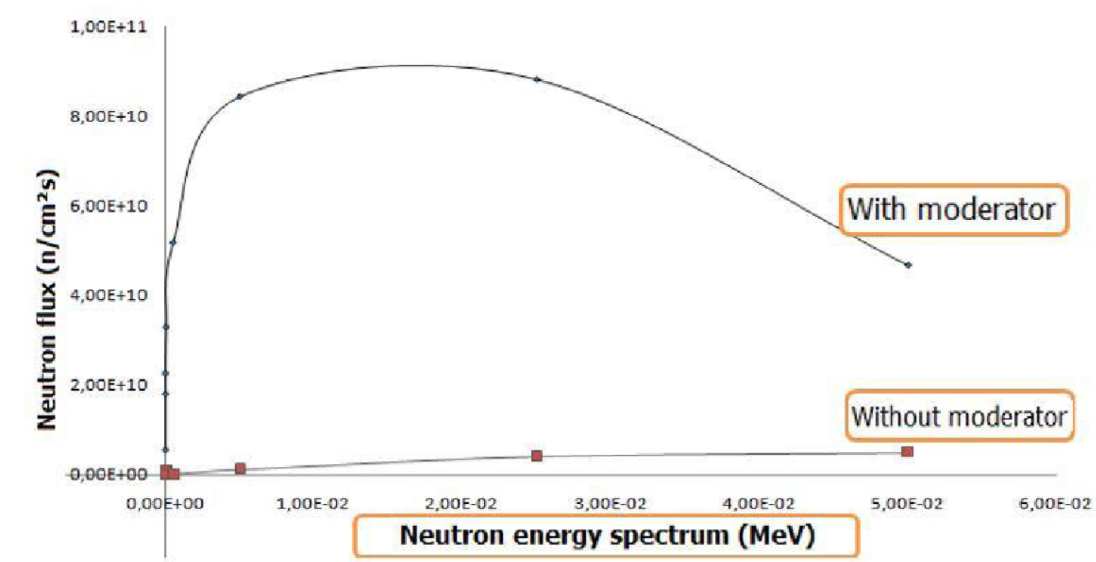

Figure 3. Neutron flux profile with moderate and non-moderate cases at low energy for target Pb.

The variation of the thermal flux profile produced by the Lead target gives the results mentioned in Figure 3. The thermal zone is not well-defined, so we thought about to realize another energy discretization in the thermal zone as indicated, in Figure 4. First, note that the neutron flux in the case of the moderator in the way that the large production of thermal flux on the contrary, to the absence of moderator the curve in red the zero flux over the thermal zone.

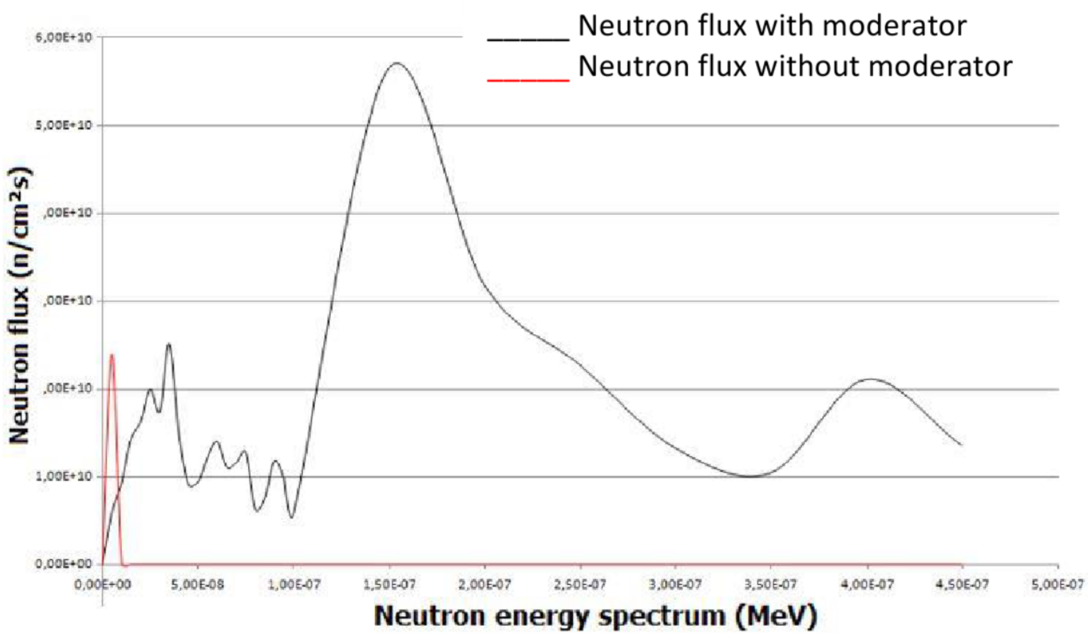

Figure 4. Neutron flux profile with moderate and non-moderate cases at low energy for target Pb.

The neutron simulation of an accelerator base electron using the Lead target for produce fast neutrons, which are moderate by a cylinder filled with water placed directly on the upper face of the target; simulation using the MCNP-6 code gives the results shown in Table 1: the variation of flux as a function of thickness. Note that the thermal flux of neutron and the thermal rate increase in the moderator along with the thickness, until the thickness equal to 4 cm (2.97×10^{10} n/cm^{2}s), after the flux begins to decrease until arriving at the value of (1.77×10^{10} n/cm^{2}s). Note also that the very high epi-thermal flux rate, which reaches 72.25 % which explains why most of the flux was at a very high energy, by the successive interactions of the neutrons with the hydrogen atoms they lose their energy, in addition, the fast neutron decreased to 24.25 %.

Table 1.
Neutron flux distribution as a function of moderator thickness for the Pb target with an accelerator base electron.

Thickness (cm)	Thermal Neutron	Epithermal Neutron	Fast Neutron	Total Neutron	Thermal flux percentage	Epithermal flux percentage	Fast flux percentage
1	2.05E+10	6.49E+11	3.81E+11	1.05E+12	1.95%	61.83%	36.23%
2	2.59E+10	6.94E+11	2.72E+11	9.92E+11	2.61%	69.93%	27.46%
3	2.91E+10	6.68E+11	2.34E+11	9.31E+11	3.13%	71.74%	25.13%
4	2.97E+10	6.13E+11	2.06E+11	8.49E+11	3.50%	72.25%	24.25%
5	2.80E+10	5.44E+11	1.85E+11	7.56E+11	3.70%	71.89%	24.41%
6	2.40E+10	4.61E+11	1.64E+11	6.50E+11	3.69%	70.99%	25.32%
7	1.77E+10	3.54E+11	1.37E+11	5.09E+11	3.48%	69.66%	26.86%

Figure 5 represents the neutron flux distribution as a function of moderator thickness, the fast-flux decreases with increasing the thickness, whereas the thermal flux increases as a function of thickness.

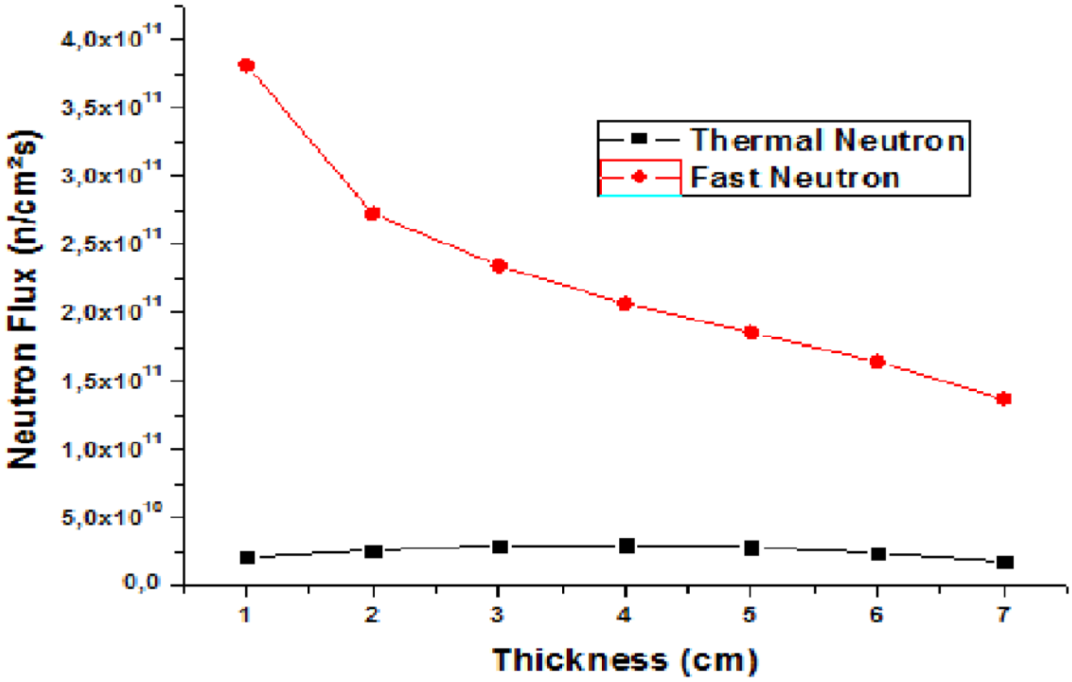

Figure 5. Distribution of thermal and fast neutron fluxes produced by the target Pb.

In order to visualize the changes in the thermal flux as a function of the thickness, we have shown in Figure 6 that the thermal neutron flux increases with a thickness of up to 4 cm with a value of (2.97×10^{10} n/cm^{2}s), after it undergoes a decrease.

The neutron flux distribution (thermal, epi-thermal and fast) by the meshing method as illustrated in Figure 7. On the way that the flux includes a small change

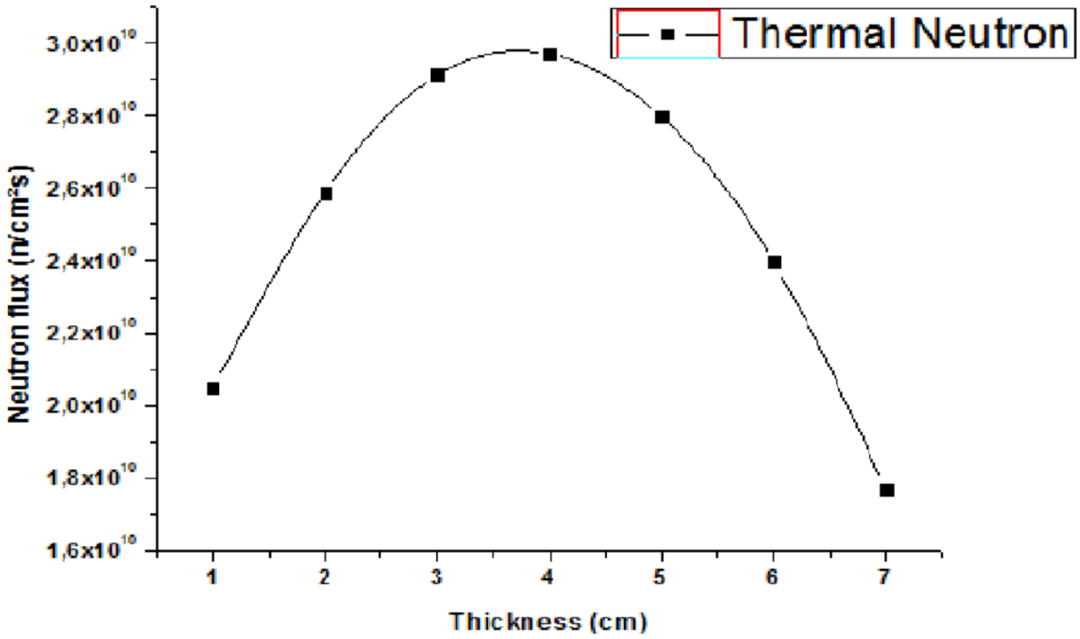

Figure 6. Flux of thermal neutrons as a function of the thickness of the target Pb.

in comparison with the other neutron mesh, treat in an article that explains the neutron distribution, this time a short color change, almost homogeneity of flux, a fast flux variation with thermal flux and epi-thermal.

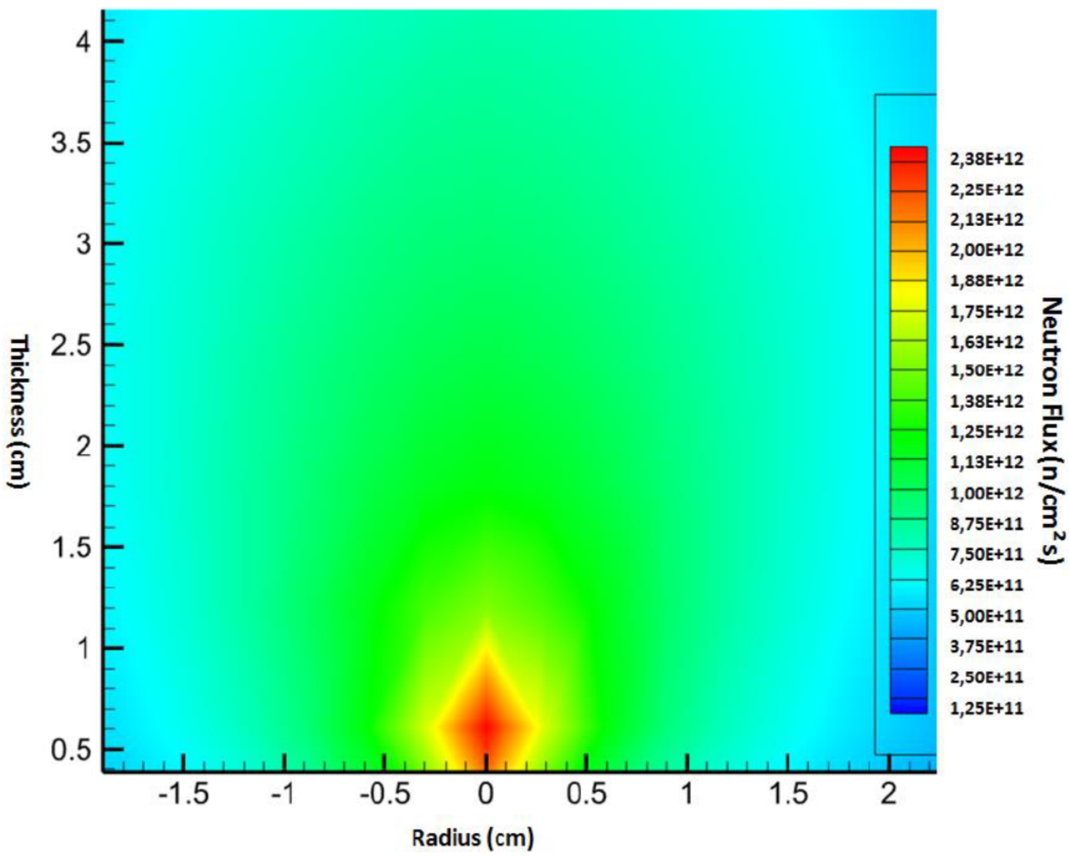

Figure 7. Thermal and fast flux radial distribution generated by the target Pb.

The thermal neutron flux generated by the Tantalum target

The present graph represents the neutron flux with moderator and without a moderator, noting that it is less intense than the neutron flux with a moderator in the range of energy higher than 0.5 MeV, whereas in the zone less than 0.1 MeV the flux with Moderator is more abundant, figure 8.

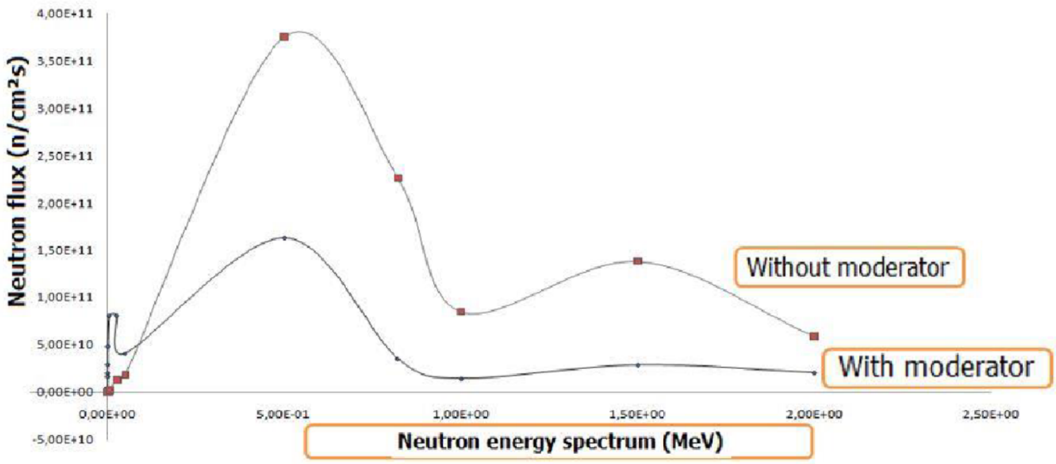

Figure 8. Neutron flux profile in the moderate case and without moderation as a function of energy for the Ta- target.

According to the previous figure, it is noted that the neutron flux is more intense with moderation in the zone of less than 0.1 MeV, for this we have discretized this energy zone to reduce it, on the way that the moderate flux superior to the flux without a moderation in the thermal zone less than 0.05 MeV, figure 9.

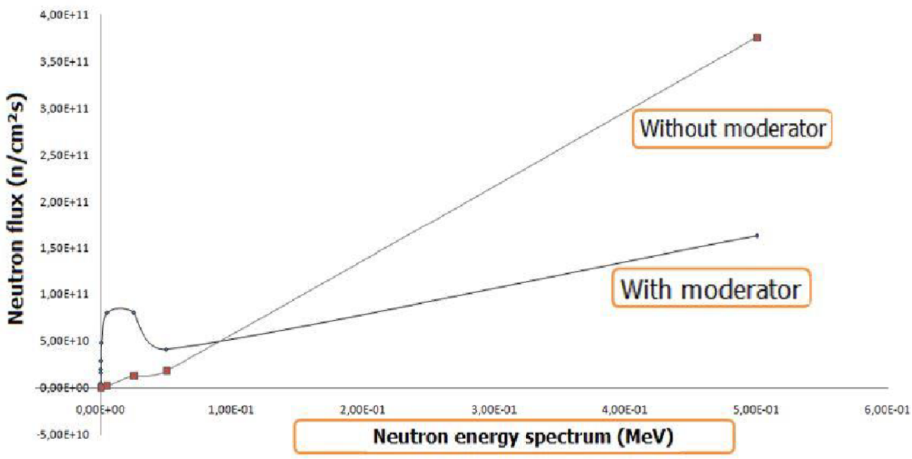

Figure 9. Neutron flux in the moderate case and without moderation as a function of energy for the Ta-target.

Figure 10 represents another discretization in the thermal domain where we have sub- groups of energy between 0 and 5×10^{-7} MeV, noting. On the one hand, that the thermal flux in the case without moderation is zero, on the other hand, the thermal flux in moderation is more intense over the entire thermal region.

The neutron distribution and the percentage of the flux (fast, epi-thermal and thermal) as a function of the thickness of the moderator are shown in Table 2,

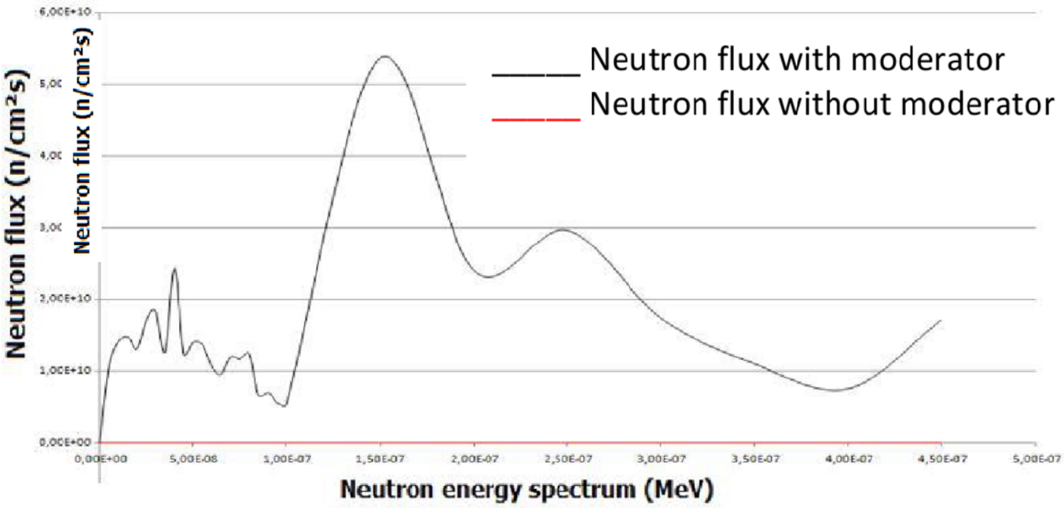

Figure 10. Neutron flux profile in the moderate and non-moderating case as a function of energy for the target Ta.

noting that the thermal flux is maximum in the case where X = 4 cm and equal to $(2.83 \times 10^{10}\ n/cm^2 s)$.

Table 2.
Neutron flux distribution as a function of moderator thickness for the Ta target with an accelerator base electron.

Thickness (cm)	Thermal Neutron	Epithermal Neutron	Fast Neutron	Total Neutron	Thermal flux percentage	Epithermal flux percentage	Fast flux percentage
1	1.89E+10	7.53E+11	2.36E+11	1.01E+12	1.87%	74.55%	23.37%
2	2.51E+10	6.97E+11	1.81E+11	9.03E+11	2.78%	77.19%	20.04%
3	2.78E+10	6.34E+11	1.60E+11	8.22E+11	3.38%	77.13%	19.46%
4	2.83E+10	5.65E+11	1.45E+11	7.38E+11	3.83%	76.56%	19.65%
5	2.66E+10	4.94E+11	1.32E+11	6.53E+11	4.07%	75.65%	20.21%
6	2.28E+10	4.20E+11	1.18E+11	5.61E+11	4.06%	74.87%	21.03%
7	1.68E+10	3.26E+11	9.67E+10	4.40E+11	3.82%	74.09%	21.98%

The graph of Figure 11 represents the rapid and thermal distribution of the flux as a function of the thickness. It is observed that the fast flux decreases slowly with the thickness, on the contrary, the thermal flux augments to a maximum at the thickness 4 cm, after which it decreases.

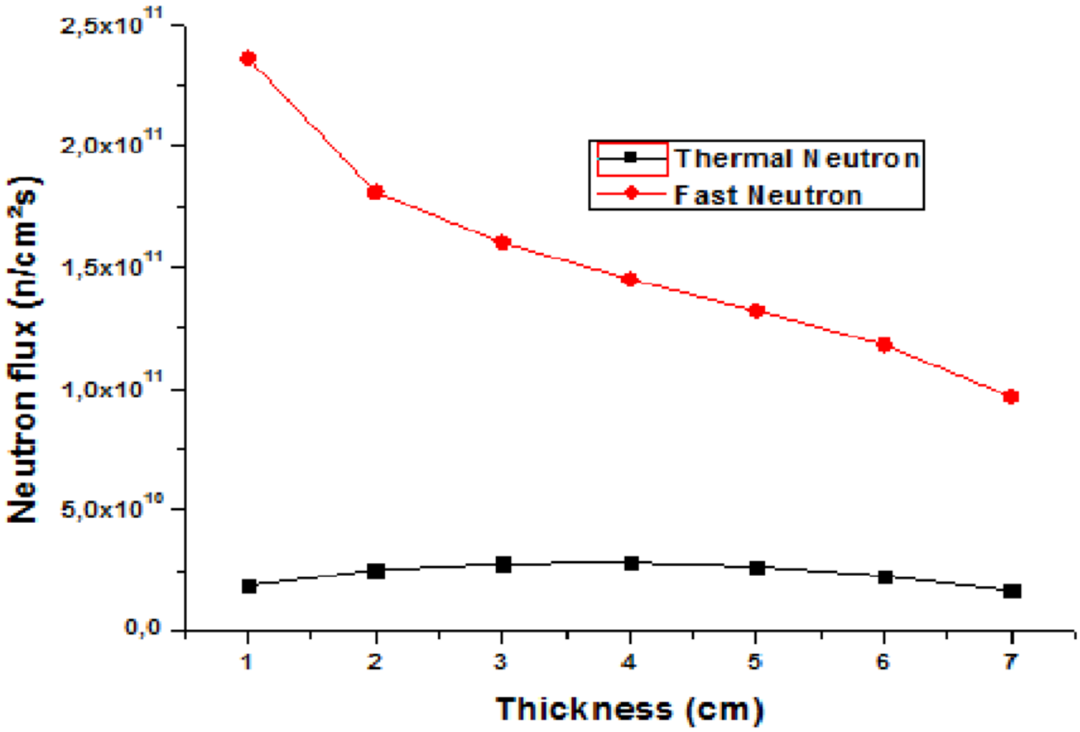

Figure 11. Thermal and fast flux distribution generated by the Ta-target.

Figure 12 shows a thermal flux capture of Figure11, which represents the thermal profile as a function of the thickness. The thermal flux increases in the moderator up to the value (2.83×10^{11} n/cm^{2}s) at the thickness of 4 cm.

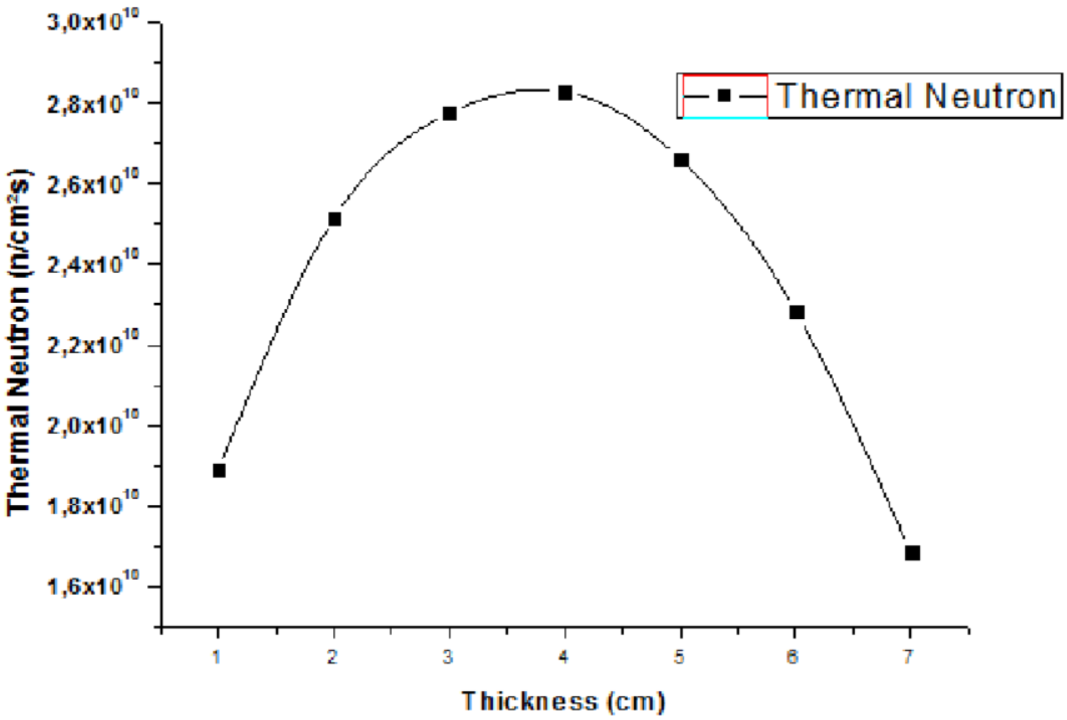

Figure 12. Thermal flux distribution generated by the Ta target.

Figure 13 represents the axial distribution of thermal flux in the moderator by the meshing method, noting that the flux varies as a function of the thickness.

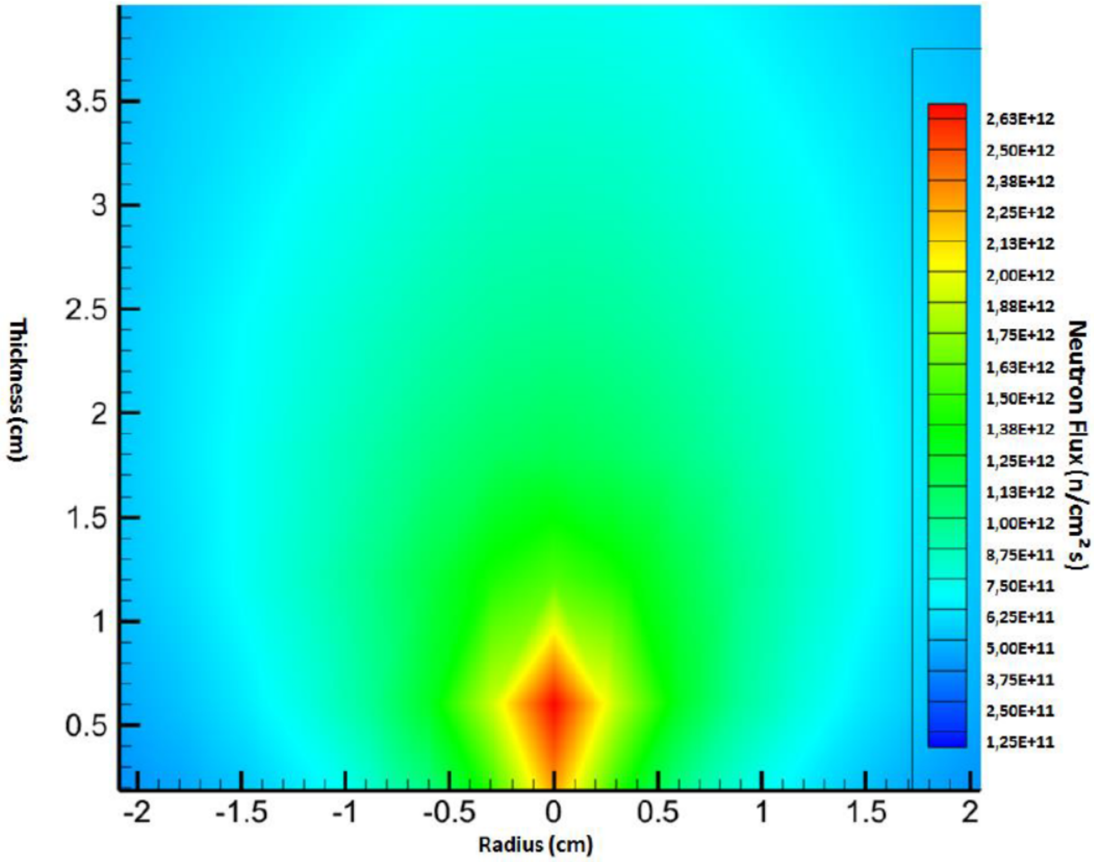

Figure 13. Radial thermal flux distribution generated by the Ta target.

Conclusion

A theoretical study of two models of calculations using the MCNP-6 code, first with the Lead target and the second with the Tantalum target. Which are driven to two different results regarding the neutron flux produced. The findings found in this study, we condense a validation of our study. We conclude that the stochastic code MCNP-6 can be used to effectively evaluate the neutron behavior of different targets. In this work, we have improved the optimal thicknesses of 4, 5 and 3 cm respectively so that the thermal neutron flux will be more intense in the moderator block that contains water. In addition, in this study, the effect of target thickness, different target materials (Ta and Pb), and proton beam energy on the neutron flux parameter was studied.

References

[1] M.A. El-Absy et-al, Sep. Purif. Technol. **71** (2010) 1-12.
[2] A.S. Elom Achoribo et.al., Appl. Rad. Isotop. **70** (2012) 76-80.
[3] O.Yu. Kochnov et al., Nuc. Ene. Tech. **1** (2015) 213-221.
[4] A. Golabian et al., Journal of Applied Radiation and Isotopes **131** (2018) 62-66.
[5] A. Didi et al., Int. J. Pharm. Pharm. Sci. **8** (2016) 327-331.
[6] A. Didi et al., Nuclear Engineering and Technology **49** (2017) 787-791.
[7] A. Didi et al., Moscow University Physics Bulletin **72** (2017) 460-464.

[8] A. Didi et al., Moscow University Physics Bulletin **72** (2017) 465-469.
[9] F. Tabbakh, Journal of Nuclear and Related Technologies **9** (2012) 17-22.
[10] V.N. Starovoitova and L. Tchelidze, Appl Radiat Isot. **85** (2014) 39-44.
[11] A. Avetisyan et al., Nuclear Medicine and Biology **47** (2017) 44-47.
[12] S. Howard et al., Applied Radiation and Isotopes **96** (2015) 162-167.
[13] K. Abbas, Nuclear Instruments and Methods in Physics Research Section A: Accelerators, Spectrometers, Detectors and Associated Equipment **601** (2009) 223-228.
[14] Z.Gholamzadeh et al., Nuclear Engineering and Technology **47** (2015) 875-883.
[15] MCNP-6. Initial MCNP6 Release Overview MCNP6 Version 1.0, Monte Carlo N–Particle Transport Code System Including MCNP6.1. Los Alamos, New Mexico: Los Alamos National Laboratory report LA-UR-13-22934 (2013).
[16] MCNP6-X. Monte Carlo N-Particle Code System for Multi particle and High Energy Application, Los Alamos, New Mexico: Los Alamos National Laboratory (2013).
[17] IAEA, Handbook of photonuclear data for applications: Cross section and spectra (TECDOC-1178, Vienna, 2000)
[18] L. Auditore et al., Nucl. Instr. Meth. Phys. Res. B**229** (2005) 137-143.
[19] A. Pazirandeh et al., Appl.Radiat. Isot. **69** (2011) 749-755.
[20] A. F. Tsechanski et al., Nucl.. Instr. Meth. Phys. Res. B: Beam Interactions with Materials and Atoms **366** (2016) 124-139.
[21] R.P. Lambert et al., Nucl.. Instr. Meth. Phys. Res. **214** (1983) 349-360.